

JOURNAL OF THE AMERICAN CHEMICAL SOCIETY

Structure of the Transition State for Hydrogen Molecule Elimination from 1,4-Cyclohexadiene

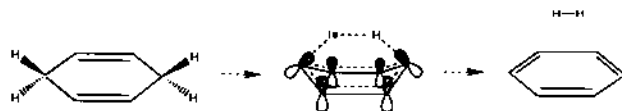
Rudolph J. Rico,^{1,3} Michael Page,^{2,4} and Charles Doubleday, Jr.⁵

Contribution from the Laboratory for Computational Physics and Fluid Dynamics, Naval Research Laboratory, Washington, D.C. 20375, and Department of Chemistry, Columbia University, New York, New York 10027. Received April 8, 1991

Abstract: Reactant, product, and transition-state regions of the potential energy surface for the dissociation of 1,4-cyclohexadiene (1,4-CHDN) to benzene and H₂ have been studied by using ab initio multiconfiguration self-consistent field (MCSCF) wave functions with STO-3G, 6-31G, and 6-31G** basis sets. At all computed levels of theory, the carbon framework of the reactant 1,4-CHDN is planar, and the transition state has a C_{2v}-symmetry boat-like conformation. The transition state is fairly *right* and is centrally located; the C-H and H-H distances are each extended by about 35-40% from their respective equilibrium values in 1,4-CHDN and H₂. At the best level of theory, the computed values for the activation barrier and reaction exothermicity for H₂ elimination are 60.1 and 9.3 kcal/mol, respectively, compared to an experimental activation energy of 43.8 and an exothermicity of 6.5 kcal/mol.

I. Introduction

In a recent and fascinating communication,¹ Cromwell, Liu, Yrakking, Kung, and Lee (CLVKL) reported translational, rotational, and vibrational state distributions for the molecular hydrogen generated in the photodissociation of 1,4-cyclohexadiene (1,4-CHDN) (eq 1). Significant as a prototype for Wood-



ward-Hoffmann allowed H₂ elimination from larger cyclic hydrocarbons, reaction 1 has a surprisingly low activation energy of 43.8 kcal/mol.² This low barrier can be attributed, in part, to the substantial stabilization of the products due to the resonance delocalization of the π system in benzene. Thus, even though two σ bonds in the reactant are being replaced with one σ bond and,

in effect, one π bond in the product, reaction 1 is nevertheless exothermic by 6.5 kcal/mol.³

CLVKL studied the distribution of energy among the degrees of freedom of the H₂ product to infer information about the nature of the potential energy surface in the vicinity of the transition state. If the H-H distance at the transition state is long, for example, then more of the 50-kcal/mol potential energy lost along the exit channel would be spent *slapping* the two H's together, being converted into vibrational energy. On the other hand, if the H-H distance at the transition state is already close to its equilibrium H₂ value, then most of the exit channel energy would be expected to be spent repelling the H₂ from the benzene-like fragment and thus would be converted into translational energy. An asymmetric transition state, in the sense of one hydrogen atom coming off ahead of the other hydrogen atom, could lead to rotational excitation of the H₂ because the hydrogen atom closer to the benzene fragment would be more violently repelled in the exit channel. The vibrational energy distribution found by CLVKL (a high

¹ONR/NRL Graduate Fellow; present address: Department of Chemistry, California Institute of Technology, Mail Code 139-74, Pasadena, CA 91125.

²Naval Research Laboratory.

³Columbia University.

[1] Cromwell, E. F.; Liu, D.; Yrakking, M. J. J.; Kung, A. H.; Lee, Y. T. *J. Chem. Phys.* 1990, 92, 3230.

[2] Benson, S. W.; Shaw, R. *Trans. Faraday Soc.* 1966, 63, 985.

[3] Cox, J. D.; Pilcher, G. *Thermochemistry of Organic and Organometallic Compounds*; Academic Press: London, 1970.

vibrational temperature of 4000 K) is characteristic of a fairly tight transition state, while the rotational energy distribution (a lower rotational temperature of 1600 K) is characteristic of a symmetric transition state, one in which the two hydrogens come off simultaneously.

The most intriguing finding of CLVKL, however, is a vector correlation between the recoil velocity and rotational angular momentum of the H₂ product implied by an analysis of the Doppler-broadened spectral line profiles.^{4,5} Physically, as described by CLVKL, this correlation corresponds to H₂ recoil from benzene with a dynamical preference for a "helicopter"-type motion in a plane parallel to the benzene. The specific features of the potential energy surface that lead to this dynamical effect are unknown.

We present here ab initio calculations of features of the potential energy surface for H₂ elimination from 1,4-CHDN. We present structures, energies, and harmonic vibrational frequencies for the reactant, transition state, and products, but our main focus is on the structure of the transition state or, more accurately, the structure of the saddle point. Is the transition state symmetric in the sense that the two hydrogen atoms act in concert? Is the transition state early or late? Is it tight or loose? Finally, does the structure of the transition state provide any hint of the unexpected dynamics inferred by the results of CLVKL?

II. Wave Functions and Basis Sets

The changes in electronic structure taking place during the course of reaction 1 can be qualitatively confined to eight electrons and eight molecular orbitals (MO's). For 1,4-CHDN, these are the two pairs of π C=C bonding and antibonding orbitals and the two pairs of σ C-H bonding and antibonding orbitals for the C-H bonds that will be severed in the reaction. For benzene and H₂, these correspond to the six π orbitals on benzene and the bonding and antibonding H-H orbital pair.

The electronic structure changes can be described by a multiconfiguration self-consistent field (MCSCF) wave function formed by including all possible singlet-spin configurations distributing the eight active electrons among the eight active MO's. There are 1764 such configurations. This 8-in-8 complete active space SCF (CASSCF)⁶ wave function provides a continuous, qualitatively correct description of the changes in the active orbitals during the course of reaction 1.

Three basis sets are used in this study: the STO-3G minimal basis set,⁷ the 6-31G split-valence basis set,⁸ and the 6-31G** split valence plus polarization basis set.^{9,10} There are, respectively, 38, 70, and 130 contracted basis functions for C₆H₈ using these three basis sets.

The electronic structure calculations were all performed using the MESA¹¹ system of programs on either the Cray XMP-24 at the Naval Research Laboratory or the Cray YMP at the Pittsburgh Supercomputing Center.

III. Structures and Vibrational Frequencies

A. 1,4-Cyclohexadiene. Early conclusions about the structure of 1,4-cyclohexadiene were in discord. At issue was whether the carbon skeleton is planar or whether it is bent in a boat-like conformation. While several spectroscopic¹²⁻¹⁵ studies were in-

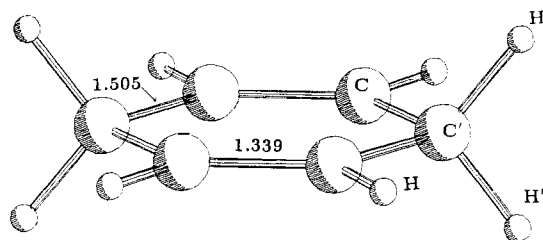


Figure 1. Structure of 1,4-cyclohexadiene calculated at the 8-in-8 CASSCF level of theory using the 6-31G** basis set.

Table I. Optimized MCSCF Structural Parameters:^a 1,4-Cyclohexadiene

	STO-3G	6-31G	6-31G**	expt ^b	exp ^c
R_{CC}	1.522	1.506	1.505	1.496	1.511
R_{CC}	1.342	1.344	1.339	1.334	1.347
R_{CH}	1.083	1.076	1.078	1.103	1.079
$R_{CH'}$	1.091	1.088	1.090	1.114	1.096
$R_{CH''}$	1.116	1.112	1.112	1.114	1.096
$\angle CC'C$	112.7	112.9	112.8	113.3	111.9
$\angle C'CC$	123.6	123.5	123.6	123.4	122.7
$\angle HCC$	120.2	119.5	119.3	123.4	118.7
$\angle H'C'H'$	105.8	104.9	105.0	103	109.8

^a Angstroms and degrees. ^b Reference 16. ^c Reference 7.

terpreted in terms of a planar structure, and one electron diffraction study suggested a planar arrangement,¹⁶ a subsequent electron diffraction study concluded¹⁷ that the molecule has a boat-like conformation, with the 1 and 4 carbon atoms 20.7° out of the plane of the four olefinic carbons. Since that time, a study of the vapor-phase far-infrared spectrum¹⁸ revealed that the molecule is either planar or has an unusually high barrier to interconversion between two equivalent boat structures (i.e., through a planar transition state). Shortly thereafter, a gas-phase Raman overtone spectrum was interpreted as being supportive of a planar structure.¹⁹ More recently, detailed analysis of earlier observed far-infrared spectra, in particular analysis of the ring-puckering and two ring-twisting modes, is consistent with a planar structure.²⁰

Theoretical calculations have fairly consistently predicted a planar (D_{2h}) structure for 1,4-CHDN. Various molecular mechanics methods, for example, have predicted planar conformations.^{15,17,21} While minimal basis set ab initio calculations at the Hartree-Fock level,²² (but with incomplete geometry optimization) have predicted a boat conformation, complete geometry optimization at the same level of theory leads to a planar structure.²³ More recent ab initio Hartree-Fock calculations²⁴ using a double-zeta quality basis set and with complete geometry optimization predict a planar conformation.

We have optimized the structure of 1,4-CHDN at the 8-in-8 CASSCF level of theory with the STO-3G, 6-31G, and 6-31G** basis sets. All three levels of theory agree with the wealth of experimental and theoretical information in predicting a planar conformation of the carbon framework in 1,4-CHDN. The 6-

(4) Dixon, R. N. *J. Chem. Phys.* **1986**, *85*, 1866.
 (5) Hall, G. E.; Sivakumar, N.; Chawla, D.; Houston, P. L. *J. Chem. Phys.* **1988**, *88*, 1866.
 (6) Siegbahn, P. E. M.; Heiberg, A.; Roos, B. O.; Levy, B. *Phys. Scr.* **1980**, *21*, 323. Roos, B. O.; Taylor, P. R.; Siegbahn, P. E. M. *Chem. Phys.* **1980**, *48*, 152.
 (7) Hehre, W. J.; Stewart, R. F.; Pople, J. A. *J. Chem. Phys.* **1969**, *51*, 2657.
 (8) Hehre, W. J.; Ditchfield, R.; Pople, J. A. *J. Chem. Phys.* **1972**, *56*, 2257.
 (9) Hariharan, P. C.; Pople, J. A. *Chem. Phys. Lett.* **1972**, *16*, 217.
 (10) Hariharan, P. C.; Pople, J. A. *Theor. Chim. Acta* **1973**, *28*, 213.
 (11) MESA (Molecular Electronic Structure Applications), copyright 1990, The University of California, by Saxe, P.; Lengsfeld, B. H.; Martin, R.; Page, M.
 (12) Gerding, H.; Haak, F. A. *Recl. Trav. Chem. Pays.-Bas.* **1949**, *68*, 293.

(13) Monostori, B. J.; Weber, A. *J. Mol. Spectrosc.* **1964**, *12*, 129.
 (14) Stidham, H. D. *Spectrochim. Acta* **1965**, *21*, 23.
 (15) Garbach, E. W., Jr.; Griffith, M. G. *J. Am. Chem. Soc.* **1968**, *90*, 3590.
 (16) Dallinga, G.; Toneman, L. H. *J. Mol. Struct.* **1967**, *1*, 117.
 (17) Oberhammer, H.; Bauer, S. H. *J. Am. Chem. Soc.* **1969**, *91*, 10.
 (18) Laane, J.; Lord, R. C. *J. Mol. Spectrosc.* **1971**, *39*, 340.
 (19) Carierra, L. A.; Carter, R. O.; Durig, J. R. *J. Chem. Phys.* **1973**, *59*, 812.
 (20) Strube, M. M.; Laane, J. *J. Mol. Spectrosc.* **1988**, *129*, 126.
 (21) Allinger, N. L.; Burket, U. *Molecular Mechanics*; American Chemical Society: Washington, DC, 1982.
 (22) Srinivasan, R.; White, L. S.; Rossi, A. R.; Epling, G. A. *J. Am. Chem. Soc.* **1981**, *103*, 7299.
 (23) Birch, A. J.; Hinde, A. L.; Radom, L. *J. Am. Chem. Soc.* **1981**, *103*, 284.
 (24) Saebo, S.; Boggs, J. E. *J. Mol. Struct.* **1981**, *73*, 137.

Table II. CASSCF/6-31G Harmonic Vibrational Frequencies (cm⁻¹)

1,4-CHDN (C _{2v})		transition state (C _{2v})		benzene + H ₂ (D _{6h})	
118	A ₁	2130i	A ₁	440 (2)	E _{2u}
384	B ₂	509	A ₂	675 (2)	E _{2g}
402	B ₁	526	A ₁	730	A _{2u}
587	A ₁	664	B ₂	754	B _{2g}
627	A ₂	695	A ₂	908 (2)	E _{1g}
669	A ₁	753	B ₁	1045 (2)	E _{2u}
736	A ₂	763	A ₁	1046	A _{1g}
900	A ₁	774	A ₁	1093	B _{2g}
954	B ₁	836	B ₂	1122 (2)	E _{1u}
1004	B ₂	948	B ₂	1134	B _{1u}
1022	A ₂	995	A ₁	1241	B _{2u}
1023	B ₁	1011	A ₂	1301 (2)	E _{2g}
1056	A ₁	1033	B ₂	1359	B _{2u}
1056	B ₁	1064	B ₁	1530	A _{2g}
1070	B ₁	1087	B ₂	1640 (2)	E _{1u}
1146	A ₂	1123	A ₁	1737 (2)	E _{2g}
1291	B ₂	1123	B ₁	3340	B _{1u}
1311	A ₂	1166	B ₂	3350 (2)	E _{2g}
1321	B ₂	1235	A ₂	3370 (2)	E _{1u}
1336	B ₂	1267	B ₁	3385	A _{1g}
1505	B ₂	1281	A ₁	4255	(H ₂)
1507	A ₂	1394	A ₂		
1536	A ₂	1403	B ₂		
1578	B ₁	1432	B ₁		
1600	A ₁	1455	A ₁		
1602	B ₁	1497	A ₂		
1776	B ₂	1569	B ₂		
1820	A ₁	1604	A ₂		
2920	A ₁	1666	B ₁		
2922	B ₁	1741	A ₁		
3170	B ₁	3347	B ₂		
3170	A ₁	3351	A ₁		
3317	A ₂	3370	A ₂		
3317	B ₁	3376	B ₂		
3342	B ₂	3392	B ₁		
3347	A ₁	3300	A ₁		
ZPE ^a	80.6	75.6		73.0	

^a Zero-point vibrational energy (kcal/mol).

31G** optimized structure is shown in Figure 1. Structural parameters for all three basis sets are presented and compared with experimental values in Table I. The general agreement is quite good, although we note that the experimental structural parameters are vibrationally averaged values and the calculated parameters are not. Because the active space of the MCSCF treats the two hydrogen atoms that will come off as H₂ differently than it treats the other hydrogen atoms, the wave function does not have D_{2h} symmetry even at planar D_{2h} geometries. Consequently, the optimized structure of 1,4-CHDN actually has C_{2v} symmetry. However, this is a small effect and should have no practical consequence: at the 6-31G level, for example, the 1 and 4 carbon atoms are 0.008 Å above the plane formed by the remaining four carbon atoms. Also, the lengths of the two C-H bonds at each of the 1 and 4 carbon atoms are not the same. The bonds that are being correlated are about 0.02 Å longer than those that are not correlated.

Harmonic vibrational frequencies and zero-point vibrational energies were computed analytically for the STO-3G and 6-31G basis sets. The 6-31G results are reported in Table II for 1,4-CHDN as well as for the transition state and the benzene (+H₂) product. The lowest frequency mode of 1,4-CHDN (118 cm⁻¹) corresponds to a symmetric flapping between equivalent boat-like conformations. If 1,4-CHDN is viewed as two ethylene molecules connected by two methylene groups, then the relative insensitivity of the energy to boat-like distortions can be attributed to the ability of the ethylene fragments to remain planar along this distortion. For a chair-like distortion, on the other hand, the ethylene fragments cannot remain planar, and the energy rises more rapidly.

Our conclusion that the planar structures for 1,4-CHDN are true local minima on the STO-3G and 6-31G potential energy surfaces is confirmed by the fact that the respective force constant

Table III. Optimized MCSCF Structural Parameters:^a Benzene and H₂

	STO-3G	6-31G	6-31G**	exp
R _{CC}	1.405	1.399	1.396	1.393 ^b
R _{CH}	1.082	1.074	1.076	1.084 ^b
R _{HH}	0.735	0.753	0.753	0.741 ^c

^a Angstroms and degrees. ^b See ref 25. ^c See ref 26.

Table IV. Optimized MCSCF Structural Parameters:^a Transition State

	STO-3G	6-31G	6-31G**
R _{CC'}	1.461	1.452	1.449
R _{CC}	1.366	1.363	1.359
R _{CH}	1.081	1.072	1.075
R _{CH'}	1.086	1.074	1.078
R _{CH''}	1.540	1.547	1.540
R _{H''H''}	0.925	1.050	1.027
∠CC'C	115.4	116.0	116.1
∠CCC'	115.1	115.5	115.5
∠HCC'	120.8	120.8	120.9
∠H'C'C	117.9	118.2	118.1
∠HCC	123.3	123.1	122.9
∠H''C'C	92.3	92.8	92.6
∠H''H''C'	123.1	120.4	120.8
∠CCC'C	42.1	40.2	40.3
∠C'CCC'	0.0	0.0	0.0
∠HCCC'	169.5	170.9	169.7
∠HCC'C	148.1	148.7	149.7
∠H'C'CC	171.0	170.7	171.2
∠H''C'CC	93.6	94.4	94.1
∠H''H''C'C	57.8	58.1	58.2

^a Angstroms and degrees.

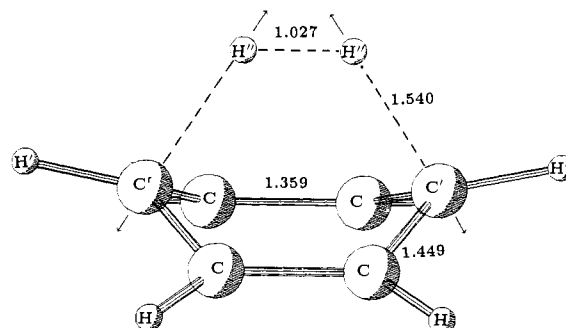


Figure 2. Structure of the transition state for H₂ elimination from 1,4-cyclohexadiene calculated at the 8-in-8 CASSCF level of theory using the 6-31G** basis set. The arrows correspond approximately to the normal mode of the single imaginary frequency.

matrices are positive definite. At the 8-in-8 CASSCF/6-31G** level, however, determination of the matrix of force constants is computationally prohibitive. Nevertheless, the fact that a Newton-Raphson optimization beginning at a slightly nonplanar geometry and using the positive definite 6-31G force constant matrix converges to a planar stationary point suggests that the 6-31G** stationary point is also a minimum.

B. Benzene + H₂. The optimized structures for benzene and H₂ at the 8-in-8 CASSCF level with the STO-3G, 6-31G, and 6-31G** basis sets are given in Table III. The 8-in-8 CASSCF wave function asymptotically leads to a 6-in-6 CASSCF description of benzene and a 2-in-2 description of H₂. The entire π system of benzene is included in the correlation treatment, and the carbon atoms are all treated equivalently. The experimental benzene structure is well-reproduced by the calculations. At the 6-in-6 CASSCF level with the 6-31G** basis set, the C-C bond length is 0.003 Å greater than experiment, and the C-H bond

(25) Langseth, A.; Stoicheff, B. P. *Can. J. Phys.* **1956**, *34*, 350.

(26) Huber, K. P.; Herzberg, G. *Molecular Spectra and Molecular Structure. IV. Constants of Diatomic Molecules*; Van Nostrand Reinhold: New York, 1979.

length is 0.008 Å less than experiment.

C. Transition State for 1,4-CHDN → Benzene + H₂. The structure of the transition state calculated at the 8-in-8 CASSCF level using the 6-31G** basis set is shown in Figure 2. Transition state structural parameters calculated at the 8-in-8 CASSCF level and using STO-3G, 6-31G, and 6-31G** basis sets are given in Table IV. All three basis sets lead to a qualitatively similar C_{2v} structure for which the carbon skeleton has a boat-like conformation.

About 200 kcal/mol of reactant chemical bonds are severed during H₂ elimination from 1,4-CHDN. Likewise, about 200 kcal/mol of product chemical bonds are formed. The observed low-energy barrier of 43 kcal/mol for this reaction indicates that, while potential energy is being lost from breaking bonds, there is effective, simultaneous stabilization energy being gained from incipient product bonds. The geometrical constraints on this simultaneous stabilization are substantial. The two hydrogens that come off as H₂ begin over 4 Å apart in 1,4-CHDN, and the 1 and 4 carbon atoms that these hydrogens are attached to begin over 3 Å apart. Yet, at the transition state, these hydrogens are about 1 Å apart. The two hydrogen atoms can be brought into close proximity expending little energy by distorting the carbon skeleton of 1,4-CHDN in a boat-like direction, because such a distortion does not disturb the planarity of the ethylene fragments in 1,4-CHDN. However, gaining H–H bond stabilization while breaking the two C–H bonds is insufficient to explain the low activation energy. There must additionally be incipient benzene resonance stabilization energy at the transition state, and this stabilization requires a nearly planar carbon skeleton to get efficient π-type overlap of the six carbon p orbitals.

The transition state structure allows the best compromise between stabilization from C–H bonding, from H–H bonding, and from π bonding in the ring. The calculated structure is *centrally* located; it favors neither 1,4-CHDN nor benzene and H₂. At the 8-in-8 CASSCF/6-31G** level, the C–H bonds that are being broken in the reaction are extended by 0.46 Å from their original length in 1,4-CHDN, while the H–H bond that is being formed is extended by 0.27 Å from its final value in H₂. These extensions are revealed as nearly equivalent when viewed in terms of their respective equilibrium bond lengths; the C–H bonds and the H–H bond are extended by 38.5% and 36.4% from their equilibrium values, respectively. Similarly, at the 6-31G level, the C–H bonds are extended by 0.43 Å (39.1%) and the H–H bond is extended by 0.30 Å (39.4%). The structure of the transition state at the minimal STO-3G basis set level, however, is skewed toward products. In particular, the H–H bond is extended by 0.19 Å from its equilibrium value, only about two-thirds of the calculated bond length extension with the 6-31G** basis set.

Another measure of the position of the transition state is the length of the C–C bonds. At the reactant 1,4-CHDN, there are four C–C single bonds of length 1.51 Å and two C–C double bonds of length 1.34 Å. In the benzene product, all C–C bonds are equivalent and are about 1.40 Å long. The C–C single bonds are thus taking on multiple bond character as the reaction proceeds, and the double bonds are losing multiple bond character. These C–C double bonds of 1,4-CHDN are losing multiple bond character not because the ethylene-like fragments become twisted in any way but rather because the π system is delocalizing onto the 1 and 4 carbon atoms. The difference in C–C bond lengths at the 8-in-8 CASSCF/6-31G** level (i.e., single bond length minus double bond length) goes from 0.17 Å (1.51 – 1.34) in 1,4-CHDN to zero in benzene. At the transition state, this difference in bond lengths is 0.09 Å, about half (46%) of the total change. The structures optimized using the two smaller basis sets share this feature. At the 6-31G level, the C–C bond length difference changes from 0.16 Å in 1,4-CHDN to 0.09 Å at the transition state, 45% of the way to benzene. With the STO-3G basis set, these numbers are 0.18 Å and 0.10 Å for 47% of the total change.

Thus from the structural behavior of the breaking C–H bonds, the forming H–H bond, and the carbon ring system, the transition state is best regarded as *centrally* located and fairly tight. The

breaking C–H bonds and the forming H–H bond are all stretched by about the same proportion (about 35–40%) of their equilibrium values. Also, about half of the ultimate changes in C–C bond lengths are realized at the transition state. This is consistent with the presence of significant resonance stabilization of the π system at the transition state.

The calculated 8-in-8 CASSCF/6-31G harmonic vibrational frequencies are presented in Table II. This vibrational analysis was done to determine a correction to the energetics for zero-point vibrational energy. But, more importantly, it was also done to verify that the located stationary point on the potential energy surface is a true saddle point. The 6-31G structure is indeed a saddle point on the potential energy surface because it has one and only one negative eigenvalue of the force constant matrix (one imaginary frequency). The STO-3G stationary point was also verified to be a true saddle point by a force constant calculation.

The symmetry of the transition state is particularly interesting in light of the observation of CLVKL that the H₂ comes off with a preference for rotation in the plane of the benzene. Such an H₂ rotation would adiabatically correlate with a *twisting* vibration at the transition state, a motion for which the H₂ twists in one direction and the ring twists in the other direction. If the structure of the transition state itself was actually distorted in such a direction instead of having C_{2v} symmetry, this would be manifested by two negative eigenvalues of the force constant matrix at the C_{2v} stationary point. One of these negative eigenvalues would correspond to motion toward products, while the other negative eigenvalue would correspond to the symmetry-breaking twisting motion mentioned above. We have identified a normal vibrational mode at the transition state that corresponds mostly to H₂ twisting. The frequency of this mode is fairly high, 1394 cm⁻¹ at the 6-31G level and 1655 cm⁻¹ at the STO-3G level. We have also identified another normal vibrational mode at the transition state that breaks C_{2v} symmetry and corresponds predominantly to a twisting of the carbon ring. At 509 cm⁻¹, this ring-twisting vibration is the lowest frequency mode at the transition state.

The highest level of theory at which we calculated a transition state structure is 8-in-8 CASSCF with a 6-31G** basis set. Unlike the similar structures calculated with the smaller basis sets, we were unable to unequivocally verify that the 6-31G** structure is a true saddle point on the potential energy surface by calculating the full matrix of force constants to show that it has one and only one negative eigenvalue. Instead, we performed a series of calculations to determine that the 6-31G** structure is indeed a true saddle point. Of concern is whether the structure is stable with respect to the twisting motion mentioned above. Ostensibly, all we have to do to verify this is twist the molecule a small amount in this direction from the C_{2v} structure. If the energy goes up, the structure is stable with respect to twisting and the C_{2v} structure is a true saddle point; if the energy goes down, the structure is not stable and true transition state is twisted. However, in practice we do not know the ideal direction for the twisting motion, and we could easily unintentionally include components of other modes for which the energy goes up. A more convincing test is to twist the molecule away from the C_{2v} stationary point, and then use the 6-31G force constants to initiate a Newton–Raphson optimization. If the C_{2v} structure was not a true saddle point, then this iterative procedure would not converge back to the C_{2v} stationary point. As a check, we first distorted the 6-31G structure—a structure that we know to be a true saddle point—by increasing the C1–C4–H''–H'' dihedral angle by 2, 15, and 30° from its C_{2v} value of 0. Each time, the optimization procedure brought the structure back to the C_{2v} saddle point. Next, we distorted the 6-31G** structure by increasing the C1–C4–H''–H'' dihedral angle from 0 to 15°. The subsequent 6-31G** optimization procedure converged back to the C_{2v} saddle point structure in much the same way as it did on the 6-31G surface. This test and the fact that the lowest frequency at the 6-31G level is as large as 509 cm⁻¹ suggest that the calculated 8-in-8 CASSCF/6-31G** structure is also a true saddle point on the potential energy surface.

Table V. Relative Energies of Reactants, Transition State, and Products (kcal/mol)

basis set	<i>N</i> ^a	1,4-CHDN	transition state	benzene + H ₂
STO-3G	38	0.0	80.3	4.9
6-31G	70	0.0	58.1	-14.3
6-31G** ^b	130	0.0	60.1	-9.3
expt ^c		0.0	43.8	-6.5

^aNumber of contracted basis functions. ^bUses 6-31G zero-point correction. ^cReference 3.

IV. Energetics

The energetics for the reaction are given in Table V. All of the values reported in the table are corrected for zero-point vibrational energy differences. The zero-point energies were determined in the harmonic approximation from the unscaled calculated vibrational frequencies. The STO-3G energetics incorporate STO-3G zero-point corrections, while the 6-31G and 6-31G** energetics incorporate 6-31G zero-point corrections. All energies were computed at the respective optimized geometries from Tables I, III, and IV.

The computed overall reaction energy improves with increasing basis set. At the STO-3G level, the reaction energy differs from experiment by 11.4 kcal/mol, and the reaction is incorrectly predicted to be *endothermic* by 4.9 kcal/mol. The error with the 6-31G basis set is in the opposite direction and is reduced to 7.8 kcal/mol. At the best level of theory (8-in-8 CASSCF/6-31G**), the reaction is predicted to be 9.3 kcal/mol exothermic, in good agreement with the experimental exothermicity of 6.5 kcal/mol.

The calculated barrier height is substantially greater than the measured activation energy of 43.8 kcal/mol at all three levels of theory. The STO-3G barrier (80.3 kcal/mol) is too high by almost a factor of 2. The results are significantly improved at the 6-31G level, for which the calculated barrier is 58.1 kcal/mol. The addition of polarization functions to the basis set raises the barrier by 2.0 kcal/mol to 60.1 kcal/mol. However, we note that polarization functions also reduce the exothermicity by 5.0 kcal/mol, bringing it closer to experiment. Therefore, the lower 6-31G barrier may just be a reflection of the 7.8-kcal/mol overestimate of the exothermicity. The 8-in-8 CASSCF/6-31G** energetics are schematically compared with experiment in Figure 3. Although the MCSCF calculations reported here properly describe the qualitative changes in the wave function associated with the breaking and forming chemical bonds, they do not include *detailed dynamical electron correlation effects, which can have a substantial effect on the energetics.* For example, in the concerted molecular dissociation of CH₂NNO₂ to HONO and HCN, two bonds are broken and two bonds are simultaneously formed, as in H₂ elimination from 1,4-CHDN. In the former case, 8-in-8 CASSCF calculations similar to those reported here yield an activation energy that is about 15 kcal/mol higher than the activation energy obtained through multireference configuration interaction calculations with the same basis set.²⁷ Although similar configuration interaction calculations are prohibitive in this case, a 15-kcal/mol dynamical electron correlation effect here would bring the calculated barrier in line with the experimental activation energy.

V. Discussion

Our conclusion from the best electronic structure calculations that we are able to do for H₂ elimination from 1,4-CHDN (a 1764 configuration MCSCF wave function with a basis set that includes polarization functions on all of the atoms) is that the transition state for the reaction is fairly tight and has C_{2v} symmetry. This result agrees with the suggestion of CLVKL from the observed small rotational excitation that the transition state is highly symmetric in the sense that both hydrogen atoms come off si-

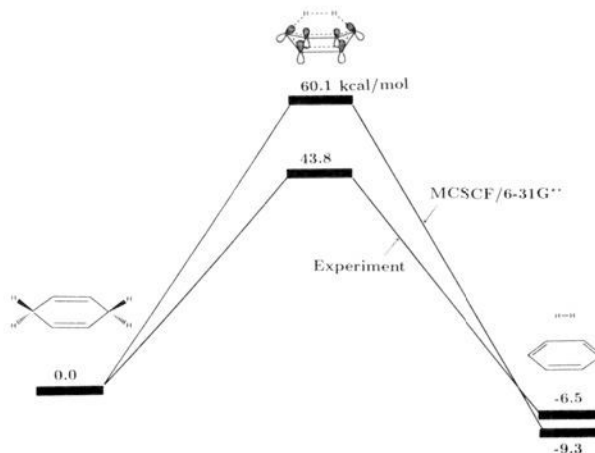


Figure 3. Comparison of energetics for H₂ elimination from 1,4-cyclohexadiene calculated at the 8-in-8 CASSCF level of theory using the 6-31G** basis set with experimental energetics.

multaneously. It also agrees with their suggestion based on the more substantial vibrational excitation that the transition state is fairly tight.

The structure of the transition state reveals nothing about the most exciting finding of CLVKL: that the H₂ comes off with a dynamical preference for a *helicopter*-type motion, i.e., rotation in a plane parallel to the benzene ring. We can, nevertheless, speculate about what features of the potential energy surface might lead to such a preference. In large part, energy available to product internal and relative motion comes from two sources: internal energy of the dissociating molecule at the transition state, which we assume to be statistically distributed among the internal degrees of freedom, and the transition-state potential energy released along the exit channel. Assuming the former is also statistically distributed among the product degrees of freedom, it is the shape of the potential energy surface in the exit channel region that is responsible for any preferential funneling of energy into specific product degrees of freedom. It is well-known, for example, that collinear atom-diatom exchange reactions (A + BC → AB + C) that have *early* barriers on the potential energy surface yield vibrationally excited AB products. This can qualitatively be viewed as a consequence of the *curvature* (change in direction) of the reaction path or valley on the way downhill from the transition state. Reaction path curvature couples motion along the steepest downhill reaction path to internal motions that are locally perpendicular to the path.²⁸

For H₂ elimination from 1,4-CHDN, initial motion along a steepest descent reaction path from the transition state toward the benzene and H₂ products involves the symmetric motion shown by the arrows in Figure 2. One of the *walls* of this reaction valley is a stable twisting motion of the H₂ moiety. If a C_{2v} reaction path is followed all the way to products, then the force constant for this twisting motion goes to zero as this mode evolves into a free rotation of the H₂ product. However, suppose that partway down the C_{2v} path, this force constant changes from positive (stable twisting vibration) to negative (unstable motion). In other words, suppose the initial C_{2v} reaction *valley* becomes a C_{2v} reaction *ridge*. In this case, the steepest descent path bifurcates into two equivalent paths corresponding to H₂ twisting in the two equivalent directions. On such a potential energy surface, some of the kinetic energy gained in the exit channel would be funneled into the H₂ twisting motion.

Another candidate for a symmetry-breaking mode to become unstable along the C_{2v} path is the ring-twisting vibration. This mode has a frequency of 509 cm⁻¹ at the transition state. There is, in fact, a plausible reason why this mode might become unstable along the product valley. At the transition state, the symmetric

(27) Mowrey, R. C.; Page, M.; Adams, G. F.; Lengsfeld, B. H., III *J. Chem. Phys.* **1990**, *93*, 1857.

(28) Miller, W. H.; Handy, N. C.; Adams, J. A. *J. Chem. Phys.* **1980**, *72*, 99.

(untwisted boat conformation) carbon skeleton allows for the greatest simultaneous H-H and C-H bonding. Partway down the product valley, the burden shifts away from the C-H bonding and toward H-H bonding and π bonding in the ring. For a benzene fragment bent into a boat-like conformation, it may be energetically favorable to approach planarity by first twisting to obtain two 3-carbon atom groups with allylic-type resonance stabilization. If the bent benzene fragment wanted to twist to enhance resonance stabilization, then the leaving H_2 would ex-

perience a torque that would excite rotation in the plane of the carbon skeleton.

Acknowledgments. This research was supported by the Office of Naval Research through the Naval Research Laboratory and by the National Science Foundation. R.J.R. acknowledges support through the Office of Naval Research Graduate Fellowship Program.

Registry No. 1,4-Cyclohexadiene, 628-41-1.

Relative Basicities of the Oxygen Sites in $[V_{10}O_{28}]^{6-}$. An Analysis of the ab Initio Determined Distributions of the Electrostatic Potential and of the Laplacian of Charge Density

Jean-Yves Kempf,[†] Marie-Madeleine Rohmer,[§] Josep-Maria Poblet,[†] Carles Bo,[†] and Marc Bénard*[§]

Contribution from the Laboratoire de Chimie Quantique, U.P.R. 139 du CNRS, Université Louis Pasteur, F-67000 Strasbourg, France, the Departament de Química, Universitat de Barcelona, 43005 Tarragona, Spain, and the Laboratoire de Résonance Magnétique Nucléaire et Modélisation Moléculaire (RM3), U.R.A. 422 du CNRS, Université Louis Pasteur, F-67000 Strasbourg, France. Received June 27, 1991

Abstract: An ab initio SCF wave function has been generated for the ground state of the $[V_{10}V_{28}]^{6-}$ ion, with a basis set of triple-zeta quality for the valence shell of oxygen. This wave function has been the starting point for theoretical studies on the relative basicities of the six external oxygen sites of the title ion in order to interpret the experimental findings concerning the preferred sites of proton fixation. The topology of the distribution of electrostatic potentials (ESP) around the ion is deduced from the determination of $V(r)$ in some specific planes and on spherical surfaces centered on each of the six oxygen sites. Several ESP minima not equivalent by symmetry have been characterized, most of them, but not all, lying in the vicinity of a specific oxygen atom. The two deepest nonequivalent ESP minima are associated with the two distinct sites, referred to as O_B and O_C , undergoing protonation in $[H_3V_{10}O_{28}]^{3-}$. An analysis of the Laplacian of the charge density shows that the direction of the maxima in $-\nabla^2\rho$ which characterize local charge concentrations around the oxygen atoms, coincides within a few degrees with the direction of the ESP minima when existing, and with that of the protons in $[H_3V_{10}O_{28}]^{3-}$ in the vicinity of sites O_B and O_C .

1. Introduction

The problem we are interested in the present article originated in an experimental investigation by Day and co-workers on the title ion.¹ These authors noticed that the closest packed surface of the $[V_{10}O_{28}]^{6-}$ ion consists of a highly congested nine-atom array centered around oxygen site B (Figures 1 and 2). This surface is particularly appealing to study the conditions that decide the fixation mode of inorganic, organometallic, or organic groups to one or several oxygen atoms. In order to delineate the factors, including steric congestion, that influence those incorporation processes,² it was necessary to decide first what oxygen on the surface is basic enough to serve as a bonding site for small cationic groups. The crystal structure of $[H_3V_{10}O_{28}]^{3-}$ (**1**) was then determined by Day et al. with sufficient accuracy to locate the protons.¹ In the same work, the position of the protons was also assigned in $[H_2V_{10}O_{28}]^{4-}$ (**2**, crystal), and the predominant protonation site was determined in $[HV_{10}O_{28}]^{5-}$ (**3**, aqueous solution). Eventually, this study proved to be inconclusive in determining unambiguously the most basic oxygen site on the surface of $[V_{10}O_{28}]^{6-}$. The protonation sites in $[H_3V_{10}O_{28}]^{3-}$ (two C sites surrounding one B oxygen and leading to hydrogen-bound dimers (Figure 3)) and those in $[H_2V_{10}O_{28}]^{4-}$ (two oxygen C sites opposite with respect to the center of symmetry) are not consistent with going from **1** to **2**, through a single deprotonation. A similar

change in the protonation sites occurs between **2** and **3**, suggesting that protonation induces a nonlocal charge reorganization modifying the scale of basicities of the unperturbed $[V_{10}O_{28}]^{6-}$ ion.¹ However, a former determination of protonation sites in $[V_{10}O_{28}]^{6-}$ by ^{17}O nuclear magnetic resonance led to the conclusion that O_B is the predominant protonation site whereas O_C is protonated to a lesser extent.³ The goal of the present work is a quantitative determination of this scale of basicities on the six external sites of $[V_{10}O_{28}]^{6-}$ through an investigation of the three-dimensional distribution of the electrostatic potential (ESP), defined in every point of space as

$$V(r) = \sum_A \frac{Z_A}{|r - R_A|} - \int \frac{\rho(r')}{|r - r'|} dr' \quad (1)$$

where Z_A represents the nuclear charge of atom A, and $\rho(r')$ corresponds to the molecular electron density functional, determined from an ab initio SCF wave function. The gradient and Laplacian distributions of the computed electron density have also been derived and analyzed in connection with the ESP minima and with the X-ray determined orientation of the protons in $[H_3V_{10}O_{28}]^{3-}$.

(1) Day, V. W.; Klemperer, W. G.; Maltbie, D. J. *J. Am. Chem. Soc.* **1987**, *109*, 2991.

(2) (a) Besecker, C. J.; Day, V. W.; Klemperer, W. G.; Thompson, M. R. *J. Am. Chem. Soc.* **1984**, *106*, 4125. (b) Day, V. W.; Klemperer, W. G.; Schwartz, C. *Ibid.* **1987**, *109*, 6030.

(3) Klemperer, W. G.; Shum, W. *J. Am. Chem. Soc.* **1977**, *99*, 3544.

[†]Laboratoire RM3, Université Louis Pasteur.

[§]Laboratoire de Chimie Quantique.

[†]Universitat de Barcelona.